International Journal of Civil Engineering

Structural Engineering

Energy based structural damage index based on nonlinear numerical simulation of structures subjected to oriented lateral cyclic loading

Kabir Sadeghi*

Received: January 2010, Revised: May 2011 , Accepted: June 2011

Abstract

An energy based damage index based on a new nonlinear Finite element (FE) approach applicable to RC structures subjected to cyclic, earthquake or monotonic loading is proposed. The proposed method is based on the evaluation of nonlinear local degradation of materials and taking into account of the pseudo-plastic hinge produced in the critical sections of the structure. A computer program is developed, considering local behavior of confined and unconfined concretes and steel elements and also global behavior and damage of reinforced concrete structures under cyclic loading. The segments located between the pseudo-plastic hinges at critical sections and the inflection points are selected as base-models through simulation by the proposed FE method. The proposed damage index is based on an energy analysis method considering the primary half-cycles energy absorbed by the structure during loading. The total primary half-cycles absorbed energy to failure is used as normalizing factor. By using the proposed nonlinear analytical approach, the structure's force-displacement data are determined. The damage index is then calculated and is compared with the allowable value. This damage index is an efficient means for deciding whether to repair or demolish structures after an earthquake. It is also useful in the design of new structures as a design parameter for an acceptable limit of damage defined by building codes. The proposed approach and damage index are validated by results of tests carried out on reinforced concrete columns subjected to cyclic biaxial bending with axial force.

Keywords: Numerical simulation, Reinforced concrete, Earthquake, Cyclic loading, Damage index.

1. Introduction

During their service life, structures accumulate damages resulting from the actions of various environmental cyclic loading and impacts. The cumulative damage causes changes in the properties of the structural system, especially in case of an earthquake. The use of a damage index (D) enables the quantification of the structural damage caused by earthquakes for each structural element.

Existing damage indices are based on different characteristics such as the number of cycles (Palmgrem-Miner, Shah, Oh and Chung), stiffness (Lybas, Roufaiel and Meyer), ductility (Park, Gupta, Bertero) and energy (Banon, Darwin, Park, Meyer [1, 2] and Sadeghi [3, 4, 5]).

Within the energy based damage indices, the damage index proposed by Meyer [1, 2] is oversensitive to the number of cycles and is, therefore, not applicable in case of loading comprising repeated cycles. Meyer's "D" is criticized by the author [3, 5], Garstka [6] and Fardis [7]. The damage index recently proposed by Amziane [8] is applicable to reinforced concrete (RC) structures under uniaxial bending with axial load. It is not applicable for biaxial bending moment with axial loading cases.

The damage index and the numerical simulation approach proposed in this paper are applicable to RC structures subjected to oriented lateral cyclic loading (in any direction) which occurs in the earthquake cases.

The analysis of the reinforced concrete sections under biaxial bending with axial loading generally has the following computational aspects:

Among several existing techniques, two of them are the most common; direct search procedure to obtain either the strain equilibrium plane, or the location and inclination of the neutral axis. The first one can be used under any loading

* *Corresponding Author: ksadeghi@gau.edu.tr*
Associate Professor, Engineering Faculty, Girne American University, Girne, North Cyprus, via Mersin 10, Turkey

mode; the second can be applied only in the monotonic loading case.

The direct search procedure may be divided into three approaches. Except the case of the linear approach where exact integration rules can be used, the section is generally divided into parallel layers rotating with the neutral axis. Another way consists in dividing the cross section into fixed finite rectangular elements. In this paper a version of an imaginary domain method considering fixed finite rectangular elements (FE) is used, allowing the case of either rectangular or nonrectangular sections in the same way.

The goal of this paper is to present a method for assessment of the global damage of structures based on the local degradation of materials under cyclic loading in any direction.

2. Experimental data

The proposed damage index and related numerical simulation have been mainly validated by the experimental test results carried out at the University of Nantes [9, 10]. 20 tests were performed on columns under biaxial alternating cyclic with axial loading. The horizontal loads were applied in different horizontal directions at the top of the columns. The loading specifications for the experimental tests of six columns C0M, C45M, C0C1, C0C2, C0C3 and C45C7 as typical samples are presented in Table 1. During the tests it was observed that the experimental response of a column subjected to a 20 or 30 cycles train can be analyzed using only the first 2 cycles. The following cycles are very similar in shape [9, 10].

3. Proposed numerical simulation approach

3.1. Description of the method

The various steps needed to assess the damage on the structure due to earthquake lateral load are as follows:

- Implementing the inflection points on beams and columns for lateral loading,
- decomposing the structure to the segments positioned between the inflection points (zero moments) and critical sections (maxim moments) at joints,
- finding the shear forces at inflection points on the columns,
- analyzing the nonlinear behavior of each segment of the columns (Base Models). A segment or Base Model is a fixed bottom-free top half-column under biaxial cyclic bending moment (i.e. lateral force in any direction) with axial load which occurs during earthquake cases. To find the status of a full-scale column, the vertical loading due to dead and live loads and also the secondary moment due to P-Δ effect are assembled on the column segments.
- assembling each two connected segments for determining global behavior of each structural element to find the reduced ultimate strength of the structure element due to slenderness,
- calculation of bending moments, shear forces and axial loads at beams' ends by considering the equilibrium of connections of beam segments and column segments,
- calculation of the damage index for each structural element,
- the damage index for each structural element can be compared with acceptable damage index value, which allows decision for repair or the demolition of the structure.

3.2. Basic assumptions

In the proposed method for each concrete and reinforcement finite element (FE), a nonlinear uniaxial stress-strain relation is used and the strain distributions in sections are assumed to obey Bernoulli's kinematics law (plane sections remain plane).

The stress-strain relation of concrete and steel are expressed as nonlinear functions of strains (ε) in each (i, j) concrete and (k) steel elements (see Figure 1):

$$\sigma cc_{ij} = f(\varepsilon_{ij}) \tag{1}$$

$$\sigma c_{ij} = f(\varepsilon_{ij}) \tag{2}$$

$$\sigma s_k = f(\varepsilon_k) \tag{3}$$

For compressive confined and unconfined concrete elements the Sadeghi's cyclic stress-strain model [11] and for reinforcements the expression proposed by Park and Kent [12] based on the Ramberg-Osgood cyclic model have been used

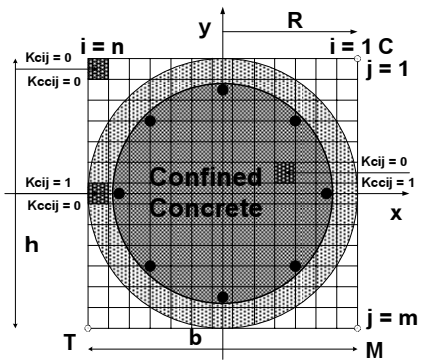

Fig. 1. Discretization of a RC member's section

Table 1. Loading specifications of some experimental tests

Column Id.	Loading Type & Angle	Axial load (kN)	Loading Conditions
C0M	Monotonic, Ω = 0°	500	Speed: 0.01 mm/sec.
C45M	Monotonic, Ω = 45°	500	Speed: 0.01 mm/sec.
C0C1, C0C2 & C0C3	Alternating Cyclic, Ω = 0°	500	20 Cycles/Amplitude
C45C7	Alternating Cyclic, Ω = 45°	500	20 Cycles/Amplitude

(see two examples in Figures 2 and 3 for confined concrete and steel elements). The concrete tensile stress is assumed to be linear up to the concrete tensile strength. For the maximum compressive strain value for unconfined concrete, the CEB code specification [13] and for confined concrete the value proposed by Sheikh [14] are used. The loss of concrete cover is taken into account.

3.3. Equilibrium conditions

The general equilibrium system of each section consists of the three nonlinear relations equating external and internal effects:

$$P_{ext} = P_{\text{int}} \tag{4}$$

$$Mx_{ext} = Mx_{\text{int}} \tag{5}$$

$$My_{ext} = My_{\text{int}} \tag{6}$$

The moment equilibrium equations (5) and (6) are written with respect to the orthogonal x and y axes passing through the centeroid of the cross-section (for a nonrectangular section, a virtual rectangular grid section is assumed) [11, 15, 16].

Detailing these previous relations leads to the following expressions:

$$P_{ext} = \sum_{i}^{n}\sum_{j}^{m} Kcc_{ij}\,\sigma cc_{ij}\,A_{ij} + \sum_{i}^{n}\sum_{j}^{m} Kc_{ij}\,\sigma c_{ij}\,A_{ij} + \sum_{k}^{ns} \sigma s_k\,As_k \tag{7}$$

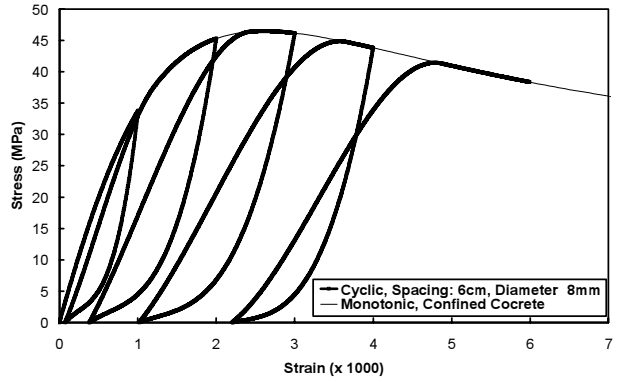

Fig. 2. An example of stress-strain curve for confined concrete

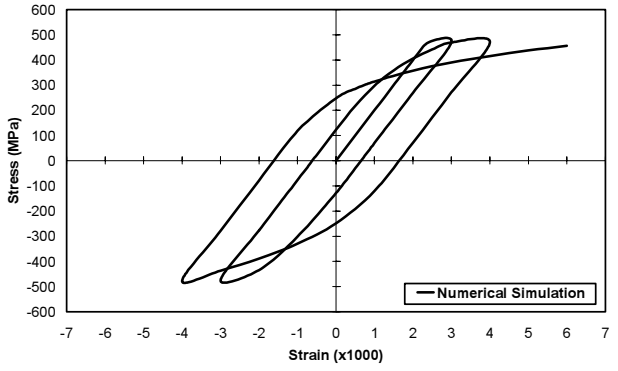

Fig. 3. An example of the stress-strain curve for a steel element

$$Mx_{ext} = \sum_{i}^{n}\sum_{j}^{m} Kcc_{ij}\,\sigma cc_{ij}\,y_{ij}\,A_{ij} + \sum_{i}^{n}\sum_{j}^{m} Kc_{ij}\,\sigma c_{ij}\,y_{ij}\,A_{ij} + \sum_{k}^{ns} \sigma s_k\,y_k\,As_k \tag{8}$$

$$My_{ext} = \sum_{i}^{n}\sum_{j}^{m} Kcc_{ij}\,\sigma cc_{ij}\,x_{ij}\,A_{ij} + \sum_{i}^{n}\sum_{j}^{m} Kc_{ij}\,\sigma c_{ij}\,x_{ij}\,A_{ij} + \sum_{k}^{ns} \sigma s_k\,x_k\,As_k \tag{9}$$

Where, Mx_{ext} and My_{ext} are the external bending moment about x and y axes; A_{ij} and A_{sk} are the concrete and steel element areas. The Kccij and Kcij factors are used to indicate whether the (i, j) element belongs to the confined concrete, unconfined concrete or an imaginary part of the section and also show the status of concrete cover. Kccij = 1, for a confined concrete element and Kcij = 1, for an unconfined concrete element. Kccij = 0 and Kcij = 0 for the other imaginary elements in the case of nonrectangular section, or for the elements when fail, ns is the total number of longitudinal reinforcement in the section, $m = i_{max}$ and $n = j_{max}$ (see Figure 1).

The strains in the concrete and steel elements can be expressed in an x-y Cartesian coordinates system as:

$$\varepsilon_{ij} = \varepsilon_0 + \phi_x.(x_{ij} - x_0) + \phi_y(y_{ij} - y_0) \tag{10}$$

$$\varepsilon s_k = \varepsilon_0 + \phi_x(xs_k - x_0) + \phi_y(ys_k - y_0) \tag{11}$$

Where, ε_0 is the strain of a point (x_0,y_0) such as section centroid; ϕ_x and ϕ_y are the curvatures in the two main axes of section: $\phi_x=(\varepsilon_C+ \varepsilon_M - 2\varepsilon_0)/b$, $\phi_y=(2\varepsilon_C+\varepsilon_T - \varepsilon_M - 2\varepsilon_0)/h$; b and h are the smaller and bigger dimensions of a rectangular section, respectively.

The coordinates of neutral axis intersections with x and y axes are found from the equations (12) and (13):

$$x_n = b/2 + (h/2)(\phi_y/\phi_x) - \varepsilon_C/\phi_x \tag{12}$$

$$y_n = h/2 + (b/2)(\phi_x/\phi_y) - \varepsilon_C/\phi_y \tag{13}$$

The basic equilibrium is justified over a critical hypothetical cross-section assuming the Navier law with an average curvature. The method used qualifies as a "Strain Plane Control Process" that requires the resolution of a quasi-static simultaneous equations system using a triple iteration process over the strains. It is based on the cyclic non-linear stress-strain relationships for concrete finite elements and reinforcements. In order to reach equilibrium, three main strain parameters ε_C, ε_T (the strains in the extreme compressive and tensile points) and ε_M (the strain in the point M located at the section corner) are used as three main variables as shown in Figure 1. For non-rectangular sections these points *C, T* and *M* may be outside the actual cross-sections and be located on the discretizing mesh frontiers).

3.4. Loading and stress-strain histories methodology

The loading history of concrete and steel finite elements on the stress-strain curves are saved and compared. This is not only related to the loading history, but also to the position of the FE on the sections. Each step of loading a segment or

concrete FE or steel FE is saved relative to the two previous steps.

3.4.1. Loading history on sections and segments

Based on $M_{ext}(k,l)$ and $\phi(k,l)$ "applied external moment and relative curvature on the section l for loading step k", the parameters *dM1* and *dM2* (in the imposed force case) or $d\phi 1$ and $d\phi 2$ (in the imposed displacement case) are defined as follows:

$$dM1 = M_{ext}(k-1,l) - M_{ext}(k-2,l) \quad or$$

$$d\phi 1 = \phi(k-1,l) - \phi(k-2,l) \tag{14}$$

$$dM2 = M_{ext}(k,l) - M_{ext}(k-1,l) \quad or$$

$$d\phi 2 = \phi(k,l) - \phi(k-1,l) \tag{15}$$

These parameters allow following up the different phases of loading history on the sections. The four different typical trajectories are as follows:

Phase 1 - Loading:

$$[dM1 \geq 0 \text{ and } dM2 > 0] \text{ or } [d\phi 1 \geq 0 \text{ and } d\phi 2 > 0] \tag{16}$$

Phase 2 - Unloading after loading:

$$[dM1 \geq 0 \text{ and } dM2 < 0] \text{ or } [d\phi 1 \geq 0 \text{ and } d\phi 2 < 0] \tag{17}$$

Phase 3 - Unloading:

$$[dM1 < 0 \text{ and } dM2 < 0] \text{ or } [d\phi 1 < 0 \text{ and } d\phi 2 < 0] \tag{18}$$

Phase 4 - Reloading after unloading:

$$[dM1 < 0 \text{ and } dM2 > 0] \text{ or } [d\phi 1 < 0 \text{ and } d\phi 2 > 0] \tag{19}$$

3.4.2. Loading history of concrete and steel FE

Each concrete or steel FE has its own proper loading history, for example, on a section, one FE may be under loading, in the same time, the other FE may be under unloading or reloading phase.

Based on $\varepsilon(k,l,i,j)$ "strain of finite element ij of section l for the step k of the loading", the parameters of $d\varepsilon 1$ and $d\varepsilon 2$ are defined as follows:

$$d\varepsilon 1 = \varepsilon(k-1,l,i,j) - \varepsilon(k-2,l,i,j) \tag{20}$$

$$d\varepsilon 2 = \varepsilon(k,l,i,j) - \varepsilon(k-1,l,i,j) \tag{21}$$

These parameters allow fixing the limits given for iteration process to research the equilibrium parameters. The four different typical phases are as follows:

Phase 1 - Loading:

$$[d\varepsilon 1 \geq 0 \text{ and } d\varepsilon 2 > 0] \tag{22}$$

Phase 2 - Unloading after loading:

$$[d\varepsilon 1 \geq 0 \text{ and } d\varepsilon 2 < 0] \tag{23}$$

Phase 3 - Unloading:

$$[d\varepsilon 1 < 0 \text{ and } d\varepsilon 2 < 0] \tag{24}$$

Phase 4 - Reloading after unloading:

$$[d\varepsilon 1 < 0 \text{ and } d\varepsilon 2 > 0] \tag{25}$$

The same procedure is used for loading history of steel FE.

3.5. Accuracy and convergence criteria

To achieve good accuracy within a reasonable calculation time, the convergence tolerances may be considered as:

$$|\Omega_{ext} - \Omega_{\text{int}}| \leq 0.1^\circ \tag{26}$$

$$|P_{ext} - P_{\text{int}}| \leq 0.001 P_{ext} \tag{27}$$

$$|M_{ext} - M_{\text{int}}| \leq 0.001 M_{ext} \tag{28}$$

Where,

$$\Omega_{ext} = Tan^{-1}(Mx_{ext} / My_{ext}), \tag{29}$$

$$\Omega_{\text{int}} = Tan^{-1}(Mx_{\text{int}} / My_{\text{int}}), \tag{30}$$

$$M_{ext} = (Mx_{ext} + My_{ext})^{1/2}, \tag{31}$$

$$M_{\text{int}} = (Mx_{\text{int}} + My_{\text{int}})^{1/2}. \tag{32}$$

3.6. Deflection calculation

Two methods are used to calculate displacements: In the first method, the equilibrium state is calculated in each cross-section discretized along the length of the segments. A double numerical integration of ϕ_x and ϕ_y is performed to evaluate the deflection. This method is rather slow and partially depends on the number of trunks selected to represent the whole segment. The second method is based on the evidence that the structural element is highly affected in the critical zone when a lateral action occurs. The main bending effect is due to the curvature registered at critical sections.

The structural element deflections are determined using the elasto-plastic relation considering the curvature and length of RC segments. After the peak value on the moment-curvature curve of critical section, very important local effects occur at the critical section where a pseudo plastic hinge appears. Once the peak has passed, curvature enhancement is concentrated at the critical zone, while in the other regions, the curvatures decrease rapidly to near zero.

3.7. Computer program

A computer program entitled "Structural Analysis and Damage Evaluation Program" (SADEP) has been developed

by the author for simulation of the degradation, damage and behavior of structures. The SADEP software deals with the numerical simulation of a reinforced concrete structural element under earthquake load in any direction or cyclic biaxial bending moment with axial loading, for rectangular or nonrectangular sections, considering the non-linear behavior of materials.

In the SADEP computer program a FEM is proposed. Each section of structure is discretized into fixed rectangular finite elements. The nonlinear response of a segment is based mainly on these finite elements at a critical section and on the location of the inflection point. For the entire structural element, deflection is evaluated using an elasto-plastic analytic formulation. The program takes into account the confining effect of the transverse reinforcement and simulates the loss of the concrete cover. It allows the determination of the local internal behavior of critical section (i.e. strains, stresses, neutral axis, moment-curvature curve, cracks positions, loss of material, …), the global external behavior (deflections) and the failure of the structural element. The SADEP program also calculates the different types of energies for negative and positive displacements (see sections 4.2, 4.3, 4.5) and the global damage based on the proposed damage index (D).

The simulated results obtained using SADEP are confirmed with the full-scale experimental results obtained by other researchers [9, 10, 12].

3.8. Some application results using SADEP

In Figure 4, the evolution of strain ε_c at the corner C of a rectangular RC section due to maximum moment capacitance of the section versus applied axial force P for three different angles of lateral loading are shown. As this figure shows, strain ε_C decreases by increasing axial force and it generally ranges from 2.4‰ to 3.7‰, therefore the 3‰ value given by ACI code for maximum strain in the design, is not valid for some combination load cases.

Figure 5 presents the axial force-moment interaction diagram of a rectangular RC section under different applied lateral force orientations. In Figure 6, the results of proposed numerical simulation and experimental test for a cyclic loading case are compared. As this figure shows there is good agreement between simulated and experimental results.

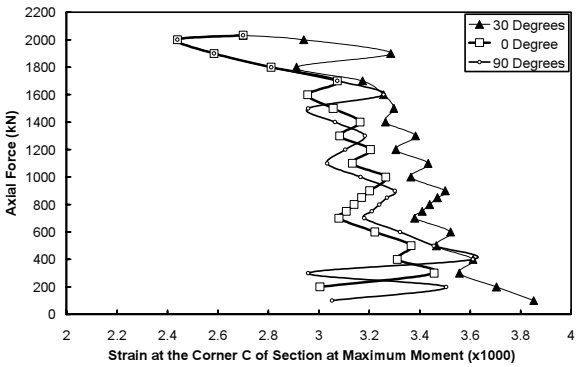

Fig. 4. Strains at the corner C of a rectangular RC section when maximum moment is applied

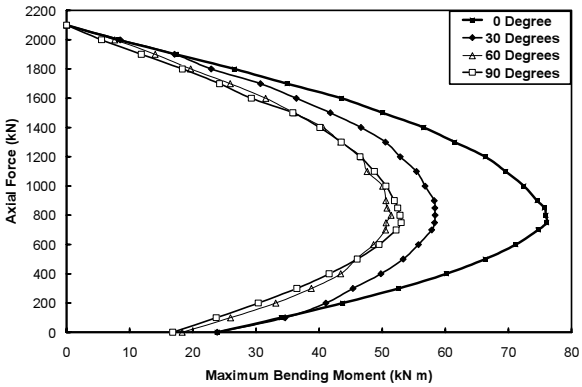

Fig. 5. Interaction diagram of a rectangular RC section under different applied lateral force orientations

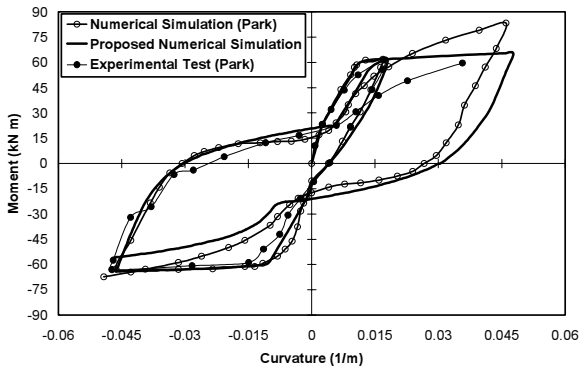

Fig. 6. Comparison of proposed model and experimental tests/simulation of Park [12]

4. Proposition of a new energy based damage index

4.1. Description of the steps

To find and evaluate the new proposed damage index, the various steps applied are as follows:

- studying the different types of energies to find the weighting, importance and the role of different types of energy in the damage index,
- evaluating the relationship between damages for displacements in positive direction, negative direction and overall damage,
- concentrating on the similarities and differences between monotonic and cyclic loading,
- studying several different normalizing factors and choosing cyclic (not monotonic) normalizing factor for cyclic loading,
- proposition of a new damage index,
- evaluation of the proposed damage index by using experimental tests results.

4.2. "Primary half-cycle" and "following half-cycle" absorbed energies

The absorbed energy is divided in two parts: the primary

half-cycle absorbed energy (E_{pi}) and the following half-cycle absorbed energy (E_{si}). Their physical meanings are described below by introducing the concepts of "primary half-cycle" (PHC) and "following half-cycle" (FHC). After Otes [17] a "primary half-cycle" is considered when any half-cycle reaches a new maximum amplitude: it is followed by a certain number of "following half-cycles" with smaller amplitudes. Whenever a certain maximum displacement $(d_{max})_i$, corresponding to the primary half-cycle $(PHC)_i$ is exceeded, a new primary half-cycle $(PHC)_{i+1}$ is established. Every PHC corresponds to a certain damage degree. For more information about practical application of the PHC and FHC absorbed energies please refer to schematic example given in Section 4.5.

4.3. Analyzing and comparing different types of energy

In order to consider the weighting, importance and the role of different types of energy in the damage index, the different energies extracted from the experimental tests and numerical simulation were analyzed and compared, as listed bellow:

- Absorbed energy "E_b" (area under the force-displacement curve. See also section 4.5).
- Dissipated energy "E_d" during cyclic loading (force-displacement hystersis loop area).
- Recovered energy "E_r" (difference between "E_b" and "E_d". See also section 4.5).
- PHC absorbed energy "E_{pi}", (see sections 4.2 and 4.5).
- FHC absorbed energy "E_{si}", (see sections 4.2 and 4.5).

In order to get a better understanding, the force and the above-mentioned energies are illustrated versus top PHC positive horizontal displacements for column C0C3 under the cyclic loading shown in Figures 7 and 8.

In the case of cyclic loading, the force-displacement envelope curve is usually close enough to the monotonic curve (see Figure 7 for results of experimental tests on C0C3 and C0M), while its maximum displacement at failure is smaller than the maximum displacement obtained monotonically but its maximum force is greater than the maximum force in monotonic case. Therefore the small difference between total PHC absorbed energy to failure ($\Sigma E_{pi}^{+)}$ in the cyclic and monotonic loading cases always stand. This can be explained basically by the different types of loading employed.

In Figure 8 the absorbed, dissipated, recovered and PHC absorbed energies are illustrated versus top PHC positive horizontal displacements for column C0C3 under the cyclic loading. The values of PHC absorbed energy to failure for columns C0C1, C0C2, C0C3, C45C7 (under cyclic lateral loading oriented in angles 0° and 45°) and C0M, C45C7 (under monotonic loading oriented in angles 0° and 45°) are reported in Table 2. As shown in Table 2, the values of ΣE_{pi}^{+} for the cyclic and monotonic loading are close to each other. In Figure 9 the PHC absorbed energies for columns C0C3 and C0M under the cyclic and monotonic loading are illustrated versus top PHC positive horizontal displacements.

Within the range of energies studied, the PHC absorbed energy calculated for cyclic and monotonic loading cases, are very similar. A quasi-linear relationship connecting the PHC absorbed energy to the PHC positive displacements for cyclic and monotonic loading can be observed as shown in Figures 8 and 9. The ratio $\Sigma E_{si}^{+}/\Sigma E_{pi}^{+}$ is approximately equal to 185. This is one of the reasons that the FHC absorbed energy effect should be considered only implicitly (not directly) or with a big reduction factor, and the damage index proposed by Mayer is not valid in the case of repeated cyclic loading.

Since the experimental tests results indicate that the damage on the structural elements is caused mainly due to the primary half-cycles, the PHC absorbed energy is emphasized and used as the key element in the damage index proposed by the author.

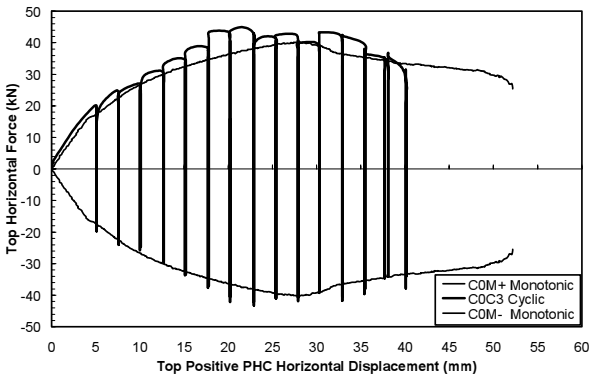

Fig. 7. Force vs. positive PHC displacement, cyclic and monotonic loading

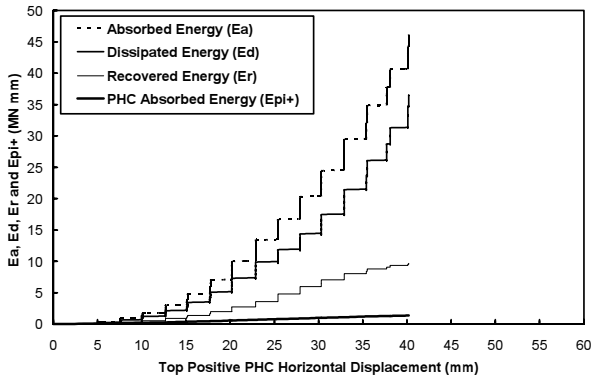

Fig. 8. Different energies versus top amplitudes of column C0C3 under cyclic loading

Table 2. Values of PHC absorbed energy to failure for some columns

Column Id.	C0M	C0C1	C0C2	C0C3	C45M	C45C7
ΣE_{pi}^{+} (MN mm)	1.60	1.55	1.21	1.30	1.18	1.04

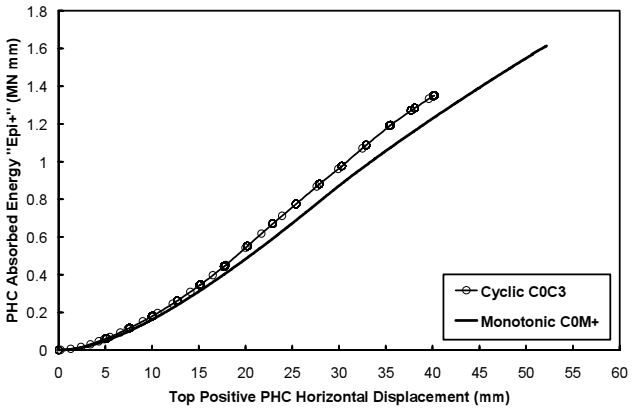

Fig. 9. PHC absorbed energy calculated for cyclic and monotonic loading

4.4. New proposed damage index "D"

The proposed damage index is simple, direct and exact at the point of failure of the structural element. In this method the summation of PHC absorbed energy to any cycle is normalized to the summation of PHC absorbed energy to failure for the same cyclic loading and on the same structural element. Since in this proposed damage index, the same cyclic loading model and structural element are used, "D" reaches exactly 100% at failure.

Based on the above mentioned analyses and processes a new damage index ("D") is proposed by the author which consists of the equations (33), (34) and (35):

$$D = \text{Max}\,[D^+, D^-] \tag{33}$$

(Unlike Meyer that considered a mathematic nonlinear relationship between damages for displacements in positive direction, negative index and the overall damage, the author has proposed a physical concept to find "D" from D^+ and D^- as given in equation (33)).

$$D^+ = \frac{\sum_{i=1}^{i=i} E_{pi}^+}{\sum_{k=1}^{k=n} E_{pk}^+} \quad \text{(for displacements in positive direction)} \tag{34}$$

$$D^- = \frac{\sum_{i=1}^{i=i} E_{pi}^-}{\sum_{k=1}^{k=n} E_{pk}^-} \quad \text{(for displacements in negative direction)} \tag{35}$$

Where i and k are the cycle numbers; n is the cycle number at structural element's failure; E_{pi}^+ and E_{pi}^- are the absorbed energies during $(PHC)_i^+$ and $(PHC)_i^-$ in positive and negative directions, respectively; ΣE_{pi}^+ and ΣE_{pi}^- are the summation of PHC absorbed energies to any cycle i; ΣE_{pk}^+ and ΣE_{pk}^- are the summations of PHC absorbed energies to failure. As examples, ΣE_{pi}^+ and ΣE_{pk}^+ which represent the areas under the force-displacement curve for positive displacements can be found from Figure 7 for two cases of cyclic and monotonic loading on columns C0C3 and C0M.

Unlike some existing damage indices (proposed by Meyer [1, 2], Sadeghi [3, 4, 5] and Garstka [6], in this new proposed damage index, monotonic loading test is not needed for the cyclic loading cases. Since in these existing damage indices, absorbed energy to failure of monotonic loading is used as normalizing factor for cyclic loading cases, some adaptation measures are required. Meyer and Garstka have fixed the extreme limits of "D" (zero and 100% at intact and failure states), but their distribution between zero and 100% especially for repeated cycles is not valid (confirmed by Garstka [6]). In the previous revision of Sadeghi's damage index, monotonic normalizing factor and an adaptation factor are used which gives a regular distribution, but the value of "D" is not exactly 100% at failure phase (e.g. "D" at failure phase, reaches 99% for C0C1, 102.7% for C0C2, 97.7% for C0C3 and 91% for C45C7. For some oriented lateral loading cases, the value of 85% is observed).

In Figure 10, the proposed "D" calculated for columns C0C1 and C0M under cyclic and monotonic loading versus top horizontal displacement are shown. As this figure indicates, in experimental test, column C0C1 is damaged during both positive and negative displacements, therefore the increasing of "D" is due to both "D^+ " and "D^- ".

In Figure 11, the proposed "D" calculated for columns C0C3 and C0M under cyclic and monotonic loading and

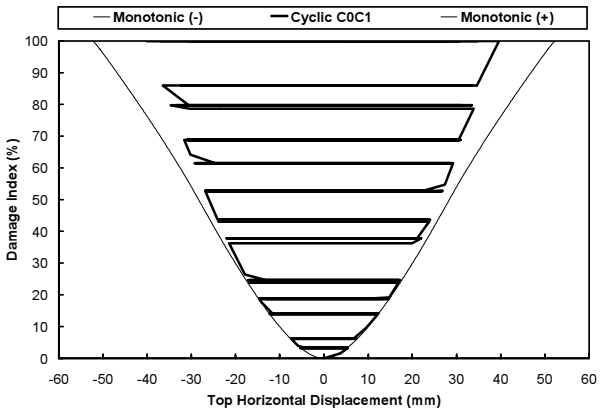

Fig. 10. Proposed Damage index, calculated for cyclic and monotonic loading, columns C0C1 and C0M

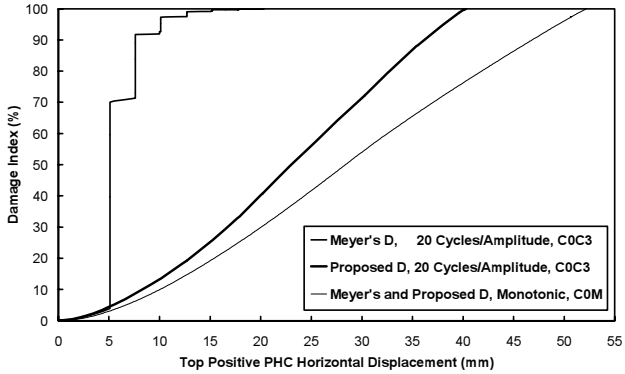

Fig. 11. Comparison of proposed and Meyer's damage indices calculated for different types of loading

Meyer's index versus top PHC horizontal displacement in positive direction are compared. As shown in this figure, the damage index proposed by Meyer is oversensitive to the number of cycles and is therefore, not applicable in case of loading comprising repeated cycles. For example, applying the column test results under cyclic loading with 20 repeated cycles per amplitude shows that Meyer's "D" reaches 70% in phase of first tension crack appearance and 99.9% in phase of compression cracks appearance.

Figures 12 and 13 represent the comparison between values of the proposed damage index calculated based on experimental tests, and numerical simulation results simulated by SADEP for monotonic and cyclic loading (C0M and C0C3). This comparison shows that for the calculation of "D", performing the expensive experimental tests is not necessary and using an analytical method such as proposed FE method is sufficient.

4.5. Schematic example for applying PHC and FHC absorbed energies in "D"

The evaluation of the PHC and FHC absorbed energies and "D" is illustrated by the following example shown schematically in Figure 14 for cyclic loading.

Figure 14 shows a typical lateral force-displacement curve for a reinforced concrete column under cyclic loading. The absorbed energy E_{p1}^{+} of the first PHC corresponds to the area under the curve of OAA', whereas E_{s1}^{+} is still zero. If point A corresponded to failure, E_{p1}^{+} would be equal to ΣE^{+}_{pimax} while i = imax = 1 and "D" = 100%. This concept retains its validity for monotonic loading at failure.

During unloading towards point B, the recovered energy corresponding to the area under the curve AA'B, is recovered, while the "D" retains its value. Following the loading cycle to the point C, is a "following half-cycle", with absorbed energy E_{s1}^{+}, corresponding to the under curve area of BCO. "$\bar{D}$" is still zero. The change in sign of E_{p1}^{+} and E_{s1}^{+} occurs at the points of symmetry about the origin of coordinate system. For the first PHC in the negative displacement range, E_{p1}^{-} is equal to the area under the curve OCDD'. The recovered energy between points D and E is not considered, and "D" retains its value. For loading between points E and F (first FHC in negative direction), E_{s1}^{-} is equal to the area under the curve EFO. Further loading in the positive direction up to point A" (maximum positive displacement to date) is equal to a new FHC. The area under the curve OFA"A' is equal to E_{s2}^{+}. After point A", a new PHC for positive displacements is formed. E_{p2}^{+} is equal to the area under the curve A"GG'A'. Subsequent cycles are analyzed with the same procedure and the damage index "D" calculated.

The proposed damage index is valid and applicable for both cyclic and monotonic loading.

4.6. Relation between different phases of damage and damage index "D"

The results of the calculation of the "D" applying the proposed index give a regular distribution of structural damages up to failure. For the cases of lateral cyclic loading applied in the direction of the main axis of section of the tested reinforced concrete columns (C0C1, C0C2 and C0C3), the average values of the proposed damage index, reached approximately 4% in the phase of the first tensile cracks appearance, 47% when the first compression cracks occurred, and 100% at failure (see Table 3).

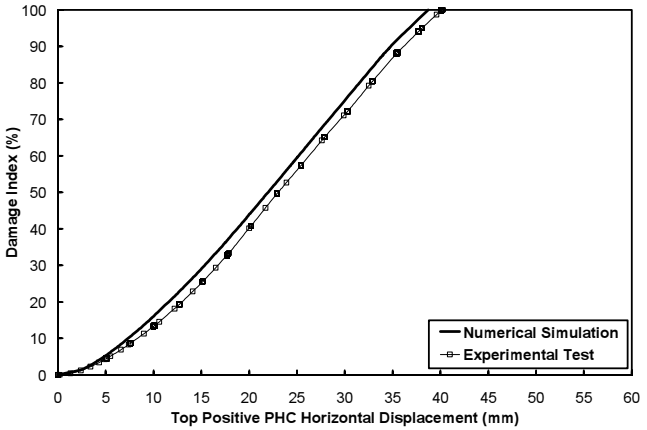

Fig. 13. "D" calculated based on experimental and numerical simulation results, cyclic loading case

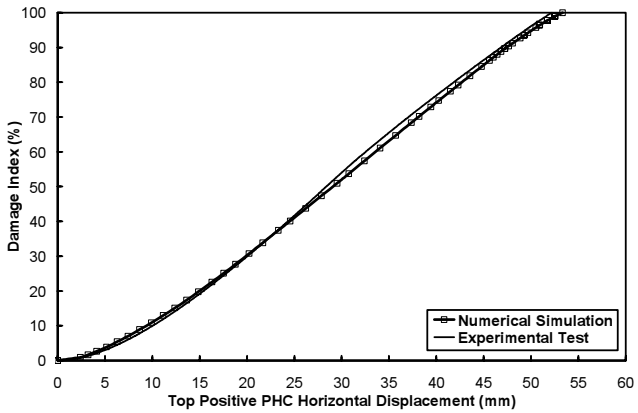

Fig. 12. "D" calculated based on experimental and numerical simulation results, monotonic loading case

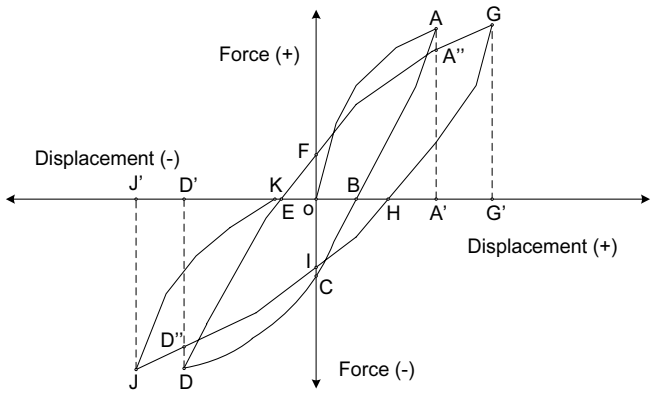

Fig. 14. Schematic illustration of damage index "D" calculation procedure for cyclic loading

Table 3. Proposed "D" values and observed damaging phases, columns C0C1, C0C2 and C0C3

Damaging Phases	Column Id.	Displacement (mm)	Damage Index (D) (%)	
	C0C1	5.3	3.19	
First tension crack	C0C2	5.1	3.66	4
	C0C3	5.0	4.56	
	C0C1	23.7	43.66	
First compression crack	C0C2	21.8	48.66	47
	C0C3	22.4	49.63	
	C0C1	39.6	100.00	
Failure	C0C2	37.8	100.00	100
	C0C3	40.2	100.00	

In order to calculate "D" the force-displacement data is required. This data can be found from numerical simulation of structures. In deciding after an earthquake, whether to repair or demolish a structure, the calculated "D" is compared with an allowable damage index ($\bar{D}$) which could be determined by technical rules and practice codes for different types of structures according to the economy and safety criteria. Further studies are required to establish allowable damage indices for important structure types such as buildings, industrial factories, marine structures, water tanks and nuclear power plants.

5. Conclusions

A nonlinear approach together with a FE program entitled SADEP has been developed by the author to simulate the behavior, the degradation and the damage of structures subjected to earthquake forces in any direction.

The energy based damage index "D" proposed in this paper is applicable to reinforced concrete structures subjected to earthquake, cyclic or monotonic (push over) loading. The proposed nonlinear numerical simulation and damage index have been validated by experimental data obtained in laboratory tests. The proposed damage index is a practical means for determining whether to repair or demolish structures after earthquake. It can also be employed in the design of new structures as a design parameter to define the acceptable limit of damage as set by building codes.

The proposed damage index reaches exactly 100% at failure, while starting from 0% at the intact state of the structure. It considers the real temporal sequence of loading cycles, gives a regular distribution adapted to different phases of damage up to failure and can be applied to RC structures under both cyclic and monotonic loading in any direction.

References

[1] Meyer, I.F.: 1988, Ein werkstoffgerechter Schaedigungsmodell und Stababschnittselement für Stahlbeton unter zyklischer nichtlinearer Beanspruchung, Technischwissenschaftliche Mitteilungen des Instituts für Konstruktiven Ingenieurbau, SFB 151 Mitteilung Nr. 88-4, Ruhr-Universitat Bochum.

[2] Meyer, I. F., Kratzig, W. B., Stangenberg, F. and Maeskouris, K.: 1988, Damage prediction in reinforced concrete frames under seismic actions." European Earthquake Engineering, 3, 9-15.

[3] Sadeghi K.: 1998, Proposition of a Damage Indicator Applied on R/C Structures Subjected to Cyclic Loading", Hirozo Mihashi & Keitetsu Rokugo (ed.), Fracture Mechanics of Concrete Structures, D-79104 Freiburg, Vol. 1, ISBN 3-931681-21-1, pp. 707-716, AEDIFICATIO Publishers, Germany.

[4] Sadeghi K., Lamirault J., & Sieffert J.G. : 1993, proposition de définition d'un indicateur de dommage", Troisième Colloque National de Génie parasismique, Génie parasismique et Aspects vibratoires dans le Génie civil", A. F. P. S, 24-26 Mars, vol. 2, Techniques Avancées, p. TA47 - TA 56, Paris.

[5] Sadeghi, K., Lamirault, J. and Sieffert, J. G.: 1993, Damage indicator improvement applied on R/C structures subjected to cyclic loading." Structural Dynamics-Eurodyn'93, Balkema, Rotterdam, ISBN 90 5410 3361.

[6] Garstka B. and Stangenberg F.: 1993, Damage Assessment in Cyclically Loaded Reinforced Concrete Members, T. Moan et al. (ed.), Structural Dynamics, vol. 1, p. 121-128, Balkema, ISBN 90 54103361, Trondheim, Norway.

[7] Fardis, M.N.,: 1994, Damage measures and failure criteria for reinforced concrete members, proceedings of 10th European conference on earthquake engineering, pages 1377-1382, 28 August-2 September 1994, Balkema (Rotterdam), ISBN: 905105321, Vienna.

[8] Sofiane Amziane and Jean Francois Dubé: 2008, Global RC Structural Damage Index Based on the Assessment of Local Material Damage, Journal of Advanced Concrete Technology, ISSN: 1346-8014, Vol. 6 , No. 3, pp.459-468.

[9] Sieffert, J.G., Lamirault, J. and Garcia, J.J.: 1990, Behavior of R/C columns under static compression and lateral cyclic displacement applied out of symmetrical planes. Structural Dynamics, Vol. 1, Kratzig et al., Balkema, ISBN 90 6191 1680, Rotterdam.

[10] Garcia Gonzalez, J.J. : 1990, Contribution á l'étude des poteaux en béton armé soumis á un cisaillement dévié alterné, Thesis of Doctorate (Ph.D.), Université de Nantes, France.

[11] Sadeghi, K. : 1995, Simulation numérique du comportement de poteaux en béton arme sous cisaillement dévié alterne, Thesis of Doctorate (Ph.D.), Université de Nantes, France.

[12] Park R, Kent D.C. and Sampson R.A.: 1972, Reinforced concrete members with cyclic loading, Journal of the Structural Division, proceeding of the American society of Civil Engineering, ST7, pp. 1341-1359.

[13] Comité Euro-International du béton : 1978, Code-Modéle CEB-FIP pour les structures en béton, Bulletin d'information no. 124-125F, Vol. 1 and 2, April, Paris.

[14] Sheikh, S.A.: 1982, A comparative study of confinement models", ACI journal, Jul.-August, pp. 296.

[15] Sadeghi, K.: 1994, Proposition of a Simulation Procedure for the Nonlinear Response of R/C Columns or Piles Under

Oriented Lateral Loading, International Journal of Engineering, Iran University of Science and Technology, vol. 5, No. 2a, pp 1-10.
[16] Sadeghi, K.: 2001, Proposition of Method of Non linear Numerical Simulation of R/C Structures under Biaxial Bending and Axial Loading, Proceedings of The First International Conference on Concrete & Development, vol. 2, PP. 233 to 239, Tehran.
[17] Otes, A.: 1985, Zur werkstoffgerechten Berechnung der Erdbebenbeanspruchng in Stahlbetontragwerken, Mitteilungen aus dem Institut für Massivbau der TH Darmstadt, Heft 25.